ELSEVIER

Powder Technology 125 (2002) 187–191

POWDER TECHNOLOGY

www.elsevier.com/locate/powtec

Electrophoresis of an insulating particle near a plane boundary

A. Sellier*

LMFA, CNRS UMR 5509, Ecole Centrale de Lyon/UCBL, 36 Avenue Guy de Collongues, BP 163, 69131 Ecully Cedex, France

Abstract

This work presents a new procedure to determine the electrophoretic motion of a solid and insulating particle $\mathscr{P}$ freely suspended in a viscous electrolyte in proximity of a plane boundary Σ. The applied electric field $\mathbf{E}_\infty$ is uniform and either parallel or normal to the plane wall. The advocated approach applies to the general case of a particle of arbitrarily smooth shape and zeta potential ζ. Our method actually rests on the treatment of seven Fredholm boundary integral equations on the particle's surface and circumvents the computation of the electric field and the electrolyte flow in the whole fluid domain. © 2002 Elsevier Science B.V. All rights reserved.

Keywords: Electrophoresis; Nonuniformly charged particle; Boundary integral equations; Wall effect

1. Introduction

We consider a rigid and charged particle $\mathscr{P}$, which is freely suspended in a viscous electrolyte of constant dielectric permittivity ϵ and viscosity μ. The surface $\mathscr{S}$ of $\mathscr{P}$ is nonconducting. Under the application of an external electric field $\mathbf{E}_\infty$, the particle experiences a rigid-body motion of unknown translational velocity $\mathbf{U}$ (which is the velocity of one point O attached to $\mathscr{P}$; see Fig. 1) and angular velocity $\boldsymbol{\omega}$. This motion, termed as electrophoresis, admits basic applications in chemical engineering and biology. Therefore, the determination of $(\mathbf{U}, \boldsymbol{\omega})$ has received considerable attention in the last decade. Within the widely employed model of the "thin double layer," the required rigid-body motion $(\mathbf{U}, \boldsymbol{\omega})$ of a single particle $\mathscr{P}$ only depends upon the ratio ϵ/μ, the external electric field $\mathbf{E}_\infty$ and the so-called "zeta potential" ζ of the particle's surface $\mathscr{S}$ (which may actually be closely related to the charged density prevailing on $\mathscr{S}$ [1]). For a single particle, the simplest theoretical result is obtained for a particle of uniform zeta potential embedded in a uniform electric field $\mathbf{E}_\infty$. Under these rather strong assumptions, the well-known Smoluchowski solution reads:

$$\mathbf{U} = \frac{\epsilon\zeta}{\mu}\mathbf{E}_\infty, \quad \boldsymbol{\omega} = 0. \tag{1.1}$$

The simple solution (Eq. (1.1)) holds for a uniformly charged (ζ uniform) particle of arbitrary shape embedded in a uniform electric field $\mathbf{E}_\infty$ [2–4]. In the electrodeposition of colloids at metallic electrodes, boundary–particle interactions may strongly affect the Smoluchowski solution for a close enough electrode. Thus, several works examine, but for a sphere of uniform zeta potential ζ only, wall effects of a plane boundary Σ (normal to $\mathbf{e}_3$; see Fig. 1) on Smoluchowski's solution. Two different cases actually occur:

Case 1. $\mathbf{E}_\infty = E\mathbf{e}_1$ is parallel to the plane boundary Σ, which is an insulating surface of uniform zeta potential ζ_w.

Case 2. $\mathbf{E}_\infty = E\mathbf{e}_3$ is normal to a conducting and plane boundary Σ of uniform electrostatic potential.

In both cases, the nonzero quantity E is either positive or negative.

As previously mentioned, several works discuss the case of the spherical particle of uniform zeta potential ζ. Case 2 has been addressed by resorting to spherical bipolar coordinates in a pioneering work by Morrison and Stuckel [5]. Using the method of reflections, Keh and Anderson [6] obtained, for both Cases 1 and 2, accurate expansions of the translational velocity $\mathbf{U}$ in terms of the ratio λ of particle radius to the distance of its center to the boundary. However, these authors assumed that the sphere translates without rotation (this assumption breaks down in Case 1). Note that Keh and Chen [7] also handled Case 1 but allowed this time a rotation of the sphere. Finally, numerical results are available in Keh and Lien [8] for Case 2.

* LADHYX, Ecole Polytechnique, 91128 Palaiseau Cedex, France. Fax: +33-1-69-33-30-30.

E-mail address: sellier@ladhyx.polytechnique.fr (A. Sellier).

0032-5910/02/$ - see front matter
PII: S0032-5910(01)00505-8

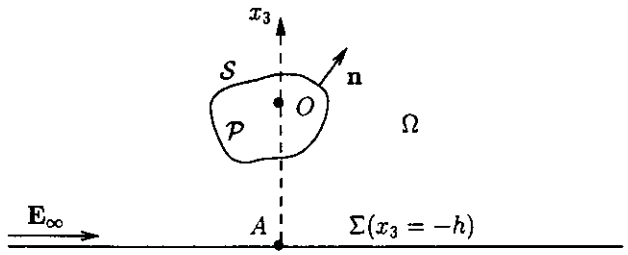

Fig. 1. A rigid particle near a plane boundary $\Sigma(x_3=-h)$ with $h>0$.

To the author's very best knowledge, the more general case of a nonuniformly charged particle of arbitrary shape has not yet been addressed. Even for a single particle, only a few papers deal with the case of a nonuniform function ζ. In this direction, one should mention the results of Anderson [9] for a single sphere of arbitrary zeta potential and the solution derived by Fair and Anderson [10] for spheroids of axisymmetric zeta potential distributions.

This paper briefly introduces a new method that makes it possible to determine the required rigid-body motion $(\mathbf{U}, \boldsymbol{\omega})$ for a particle of arbitrary shape and zeta potential ζ in both Cases 1 and 2. Only the main steps of the advocated approach and our very first numerical results are presented.

2. Governing equations

The particle $\mathscr{P}$ is rigid and freely suspended in the viscous electrolyte occupying the semi-infinite domain Ω (see the Fig. 1). Its nonconducting boundary $\mathscr{S}$ is a smooth enough surface ($\mathbf{n}$ designates the unit outwards the normal) of given zeta potential ζ. Henceforth, the usual tensor summation convention and Cartesian coordinates (O, x_1, x_2, x_3) are adopted with $\mathbf{OM}=x_i\mathbf{e}_i$. The plane boundary Σ admits the equation $x_3=-h$ with $h>0$ and is large enough (so that our particle indeed lies above the plane wall). Finally, ζ_w denotes the uniform zeta potential of the proximal boundary Σ in Case 1. The perturbation potential ϕ and the electrolyte flow $(\mathbf{u}, p)$ respectively obey the harmonic equation and the quasi-static creeping flow equations in the fluid domain [1], i.e.

$$\nabla^2\phi = 0, \quad \nabla\cdot\mathbf{u} = 0, \quad \mu\nabla^2\mathbf{u} = \nabla p \text{ in } \Omega. \tag{2.1}$$

Those equations are supplemented with the following boundary conditions [6]:

$$\nabla\phi\cdot\mathbf{n} = \mathbf{E}_\infty\cdot\mathbf{n} \quad \text{and}$$

$$\mathbf{u} = \mathbf{U} + \boldsymbol{\omega}\wedge\mathbf{OM} - \frac{\epsilon\zeta}{\mu}[\mathbf{E}_\infty - \nabla\phi] \text{ on } \mathscr{S}, \tag{2.2}$$

$$\mathbf{u} = -\frac{\epsilon\zeta_w}{\mu}[\mathbf{e}_1\otimes\mathbf{e}_1 + \mathbf{e}_2\otimes\mathbf{e}_2]\cdot$$

$$(\mathbf{E}_\infty - \nabla\phi) \text{ on } \Sigma \text{ for Case 1}, \tag{2.3}$$

$$\nabla\phi\cdot\mathbf{e}_3 = 0 \text{ on } \Sigma, \quad (\nabla\phi,\mathbf{u},p) \to \left(0, -\frac{\epsilon\zeta_w}{\mu}\mathbf{E}_\infty, 0\right)$$

$$\text{as } OM \to \infty \text{ for Case 1}, \tag{2.4}$$

$$\phi = 0 \quad \text{and} \quad \mathbf{u} = 0 \text{ on } \Sigma,$$

$$(\nabla\phi,\mathbf{u},p) \to (0,0,0) \text{ as } OM \to \infty \text{ for Case 2}. \tag{2.5}$$

Since the particle 'surface' encloses a neutral body, the electric field $\mathbf{E}_\infty$ produces zero net force and torque on $\mathscr{P}$. Thus, the net force and the torque exerted by the fluid on the freely suspended particle must vanish. One thereafter deduces six conditions for the unknown velocity components $U_j=\mathbf{U}\cdot\mathbf{e}_j$ and $\omega_j=\boldsymbol{\omega}\cdot\mathbf{e}_j$. Upon introducing, for $i\in\{1, 2, 3\}$ and $L\in\{T, R\}$, six specific Stokes flows $(\mathbf{u}_L^{(i)}, p_L^{(i)})$ of stress tensors $\boldsymbol{\sigma}_L^{(i)}$ that vanish far from the particle and fulfill the boundary conditions:

$$\mathbf{u}_T^{(i)} = \mathbf{u}_R^{(i)} = 0 \text{ on } \Sigma,$$

$$\mathbf{u}_T^{(i)} = \mathbf{e}_i \quad \text{and} \quad \mathbf{u}_R^{(i)} = \mathbf{e}_i\wedge\mathbf{OM} \text{ on } \mathscr{S}, \tag{2.6}$$

and extending to the case of our semi-infinite flow domain Ω the usual Lorentz reciprocal theorem (see Ref. [11]), one finally arrives at the key linear system:

$$K_{ij}U_j + C_{ij}\omega_j = \frac{\epsilon}{\mu}\int_{\mathscr{S}} \zeta'\,(\mathbf{E}_\infty - \nabla\phi)\cdot\mathbf{f}_T^{(i)}\,\mathrm{d}\mathscr{S}, \tag{2.7}$$

$$D_{ij}U_j + \Omega_{ij}\omega_j = \frac{\epsilon}{\mu}\int_{\mathscr{S}} \zeta'\,(\mathbf{E}_\infty - \nabla\phi)\cdot\mathbf{f}_R^{(i)}\,\mathrm{d}\mathscr{S}, \tag{2.8}$$

where $\zeta' := \zeta-\zeta_w$ for Case 1, $\zeta' := \zeta$ for Case 2, $\mathbf{f}_L^{(i)}:= \boldsymbol{\sigma}_L^{(i)}\cdot\mathbf{n}$ on $\mathscr{S}$ and

$$K_{ij} = \int_{\mathscr{S}} \mathbf{e}_j\cdot\boldsymbol{\sigma}_T^{(i)}\cdot\mathbf{n}\,\mathrm{d}\mathscr{S},$$

$$\Omega_{ij} = \int_{\mathscr{S}} [\mathbf{e}_j\wedge\mathbf{OM}]\cdot\boldsymbol{\sigma}_R^{(i)}\cdot\mathbf{n}\,\mathrm{d}\mathscr{S}, \tag{2.9}$$

$$C_{ij} = \int_{\mathscr{S}} [\mathbf{e}_j\wedge\mathbf{OM}]\cdot\boldsymbol{\sigma}_T^{(i)}\cdot\mathbf{n}\,\mathrm{d}\mathscr{S},$$

$$D_{ij} = \int_{\mathscr{S}} \mathbf{e}_j\cdot\boldsymbol{\sigma}_R^{(i)}\cdot\mathbf{n}\,\mathrm{d}\mathscr{S}. \tag{2.10}$$

Since its associated 6×6 square matrix is symmetric and negative-definite [11], the previous system (Eqs. (2.7) and (2.8)) admits, in any case, a unique solution $X=(U_1, U_2, U_3, \omega_1, \omega_2, \omega_3)$. The important message delivered by Eqs. (2.7)–(2.10) is that one only needs to evaluate the quantities $\mathbf{f}_L^{(i)}$ and $\nabla\phi$ on $\mathscr{S}$ in determining the rigid-body motion $(\mathbf{U}, \boldsymbol{\omega})$.

3. Relevant boundary integral equations

This section presents seven boundary integral equations that permit us to compute the previously alluded to the quantities on $\mathscr{S}$. Since ϕ is harmonic in Ω and obeys the boundary condition Eqs. (2.2), (2.4) and (2.5), its value on

Table 1
Normalized quantity $u_1(\lambda)$ in Case 1

λ	N=74	N=242	N=530	Keh and Chen
0.1	1.00893	1.00072	1.00012	0.99994
0.3	1.00754	0.99931	0.99872	0.99853
0.5	1.00349	0.99526	0.99467	0.99448
0.7	0.99768	0.98986	0.98933	0.98915
0.9	0.99718	0.99549	0.99790	0.99789

$\mathscr{S}$ is governed by the well-posed Fredholm boundary integral equation of the second kind:

$$-4\pi\phi(M)+\int_{\mathscr{S}}[\phi(P)-\phi(M)]\frac{\mathbf{PM}\cdot\mathbf{n}(P)}{PM^3}\mathrm{d}\mathscr{S}_P +(-1)^{j+1}\int_{\mathscr{S}}\phi(P)\frac{\mathbf{PM'}\cdot\mathbf{n}(P)}{PM'^3}\mathrm{d}\mathscr{S}_P =\int_{\mathscr{S}}[\mathbf{E}_\infty\cdot\mathbf{n}](P)\left\{\frac{1}{PM}+(-1)^{j+1}\frac{1}{PM'}\right\}\mathrm{d}\mathscr{S}_P \quad (3.1)$$

where M' $(x_1, x_2, -2h-x_3)$ denotes the symmetric of $M(x_1, x_2, x_3)$ with respect to the plane wall Σ, and the integer j refers to the addressed case (select j=1 for Case 1 and j=2 for Case 2). A numerical treatment of Eq. (3.1) makes it possible to approximate the tangential derivatives of ϕ on the surface $\mathscr{S}$ where $\nabla\phi\cdot\mathbf{n}=\mathrm{E}_\infty\cdot\mathbf{n}$. One thereafter computes the required vector $\nabla\phi$ on $\mathscr{S}$ by solving Eq. (3.1). In addition, each surface force $\mathbf{f}_L^{(i)}$ is found to satisfy the Fredholm boundary integral equation of the first kind:

$$-8\pi\mu\left[\mathbf{u}_L^{(i)}\cdot\mathbf{e}_j\right](M) =\int_{\mathscr{S}}\mathbf{G}_{jk}^h(P,M)\left[\mathbf{f}_L^{(i)}\cdot\mathbf{e}_k\right](P)\mathrm{d}\mathscr{S}_P \text{ on } \mathscr{S} \quad (3.2)$$

where $\mathbf{G}^h(P, M)=G_{jk}{}^h(P, M)\mathbf{e}_j\otimes\mathbf{e}_k$ designates the Green tensor derived by Blake [12] that vanishes on the plane boundary, i.e. $G_{jk}^h(P, M)=G_{jk}^h(M, P)=0$ as soon as P belongs to Σ. More precisely, $G_{jk}^h=G_{jk}^0+G_{jk}^1$ and G_{jk}^0, G_{jk}^1 read:

$$G_{jk}^0(P,M)=\delta_{jk}/PM+(\mathbf{PM}\cdot\mathbf{e}_j)(\mathbf{PM}\cdot\mathbf{e}_k)/PM^3, \quad (3.3)$$

$$G_{jk}^1(P,M)=-G_{jk}^0(P,M')-2c_j\left[(\mathbf{AM}\cdot\mathbf{e}_3)/PM'^3\right] \times\left\{\delta_{k3}\mathbf{PM'}\cdot\mathbf{e}_j-\delta_{j3}\mathbf{PM'}\cdot\mathbf{e}_k+\mathbf{AP}\cdot\mathbf{e}_3 \times\left[\delta_{jk}-3(\mathbf{PM'}\cdot\mathbf{e}_j)(\mathbf{PM'}\cdot\mathbf{e}_k)/PM'^2\right]\right\} \quad (3.4)$$

with $c_1=c_2=1$, $c_3=-1$ and $\mathbf{AO}=h\mathbf{e}_3$ (see Fig. 1).

Thus, one has only to solve six boundary integral equations (Eq. (3.2)) in getting the required surface forces $\mathbf{f}_L^{(i)}$ on $\mathscr{S}$.

4. Numerical method and results

Each encountered boundary integral equation, Eq. (3.1) or (3.2), is numerically solved by resorting to a standard boundary element method. More precisely, isoparametric curvilinear and triangular boundary elements are employed in discretizing $\mathscr{S}$. This results in an N-node mesh for $\mathscr{S}$. Each discretized boundary integral thereafter becomes a linear matrix system $AX=Y$ whose $N'\times N'$ square matrix is unsymmetrical and fully populated ($N'=N$ for Eq. (3.1) and $N'=3N$ for Eq. (3.2)). Finally, each dicretized linear system $AX=Y$ is solved by applying an LU factorization algorithm.

For our very first numerical results, the attention is restricted to the case of a sphere of radius $a<h$. However, the approach proposed in this work applies to any smooth enough boundary $\mathscr{S}$. Let us introduce, for our spherical particle $\mathscr{P}$, the separation parameter $\lambda<1$ as:

$$\lambda:=a/h<1. \quad (4.1)$$

We look at the dependence of the velocity components U_j and ω_j upon λ for several zeta potential functions ζ. First, we assume that ζ is uniform. As has been already addressed in previous works (see Introduction), this choice actually provides nice benchmarks in testing the accuracy of the present approach.

4.1. Case 1

In this case, $\mathbf{E}_\infty=E\mathbf{e}_1$ and $\zeta'=\zeta-\zeta_w$. The only nonzero velocity components are $U_1(\lambda)$ and $\omega_2(\lambda)$. In Table 1, comparisons of our numerical approximations against the theoretical results of Keh and Chen [7] are given for several N-node meshes on the sphere of radius a and a few values of the separation parameter λ. We actually compared the normalized quantities:

$$u_1(\lambda):=\frac{\mu U_1(\lambda)}{\epsilon(\zeta-\zeta_w)E}, \quad \Omega_2(\lambda):=\frac{a\mu\omega_2(\lambda)}{\epsilon(\zeta-\zeta_w)E}. \quad (4.2)$$

Clearly, the use of more and more refined meshes makes it possible to obtain excellent agreement with Keh and Chen [7]. The choice of N=530 nodes is seen to ensure a very good approximation in the whole range $\lambda\in[0.1, 0.9]$. If Ω_2 is seen to be highly sensitive to the separation parameter λ (see Table 2), the translational normalized velocity component u_1 exhibits a very weak sensitivity to the influence

Table 2
Normalized quantity $\Omega_2(\lambda)$ in Case 1

λ	N=74	N=242	N=530	Keh and Chen
0.1	−0.000021	−0.000019	−0.000019	−0.000019
0.3	−0.001533	−0.001535	−0.001534	−0.001535
0.5	−0.012316	−0.012336	−0.012325	−0.012333
0.7	−0.053154	−0.055069	−0.052978	−0.053007
0.9	−0.207664	−0.020722	−0.203950	−0.203891

of the wall (see Table 1). In order to track this weak dependence, it is thereafter essential to use a refined mesh on $\mathscr{S}$.

4.2. Case 2

In this case, $\mathbf{E}_\infty = E\mathbf{e}_3$ and $\zeta' = \zeta$. The only nonzero velocity component is U_3. Comparisons with the results of Keh and Lien [8] for the normalized velocity $u_3(\lambda) := \mu U_3(\lambda)/[\epsilon\zeta E]$ are listed in Table 3. Again, the 530-node mesh ensures accurate enough results.

In summary, a sphere of uniform zeta potential translates in the direction of the applied electric field $\mathbf{E}_\infty$ for any location of the proximal plane boundary. However, this simple behavior does not hold any more for a nonuniformly charged sphere! This was already obtained for a single sphere by Anderson [9]. For example, we set:

$$\zeta_1' := \frac{\zeta_0 x_1}{a}, \quad \zeta_3' := -\frac{\zeta_0 x_3}{a}, \quad u_j'(\lambda) := \frac{\mu U_j(\lambda)}{\epsilon E \zeta_0},$$

$$\Omega_j'(\lambda) := \frac{a\mu\omega_j(\lambda)}{\epsilon E\zeta_0}, \tag{4.3}$$

where ζ_0 denotes a given, uniform and nonzero zeta potential. Selecting the functions ζ_1' and ζ_3', the reader may easily check by using the material in Ref. [9] that $u_j'(0) = \Omega_j'(0) = 0$ for both Cases 1 and 2 except the normalized velocity Ω_2' that equals $-3/4$ if $\zeta' = \zeta_1$ for Case 2 and $\zeta' = \zeta_3$ for Case 1. It is now worth examining the values of our normalized velocities $u_j'(\lambda)$ and $\Omega_j'(\lambda)$ in proximity of the plane wall ($\lambda > 0$) when ζ' equals ζ_1' or ζ_3'. The 530-node surface mesh is employed and only the nonzero functions are displayed in Figs. 2 and 3.

As depicted in Fig. 2, each nonzero normalized velocity component u_j' deeply depends upon the separation variable λ in proximity of the plane boundary Σ (as $\lambda \leq O(1)$). The proximal plane is thereafter seen to induce a translation of the sphere.

If $\zeta' = \zeta_3'$, the particle translates parallel to the applied field $\mathbf{E}_\infty$. If $\zeta' = \zeta_1'$, note that the sphere translates perpendicular to the external electric field $\mathbf{E}_\infty$! The magnitude of the electrophoretic translational velocity is also seen to increase as the sphere approaches the boundary whenever ζ' does not change in the direction of $\mathbf{E}_\infty$ (symbols (○) and (●)) and to admit a maximum in other circumstances. In all cases, the proximity of the plane wall is found to

Table 3
Normalized quantity $u_3(\lambda)$ in Case 2

λ	N=74	N=242	N=530	Keh and Chen
0.1	1.00489	0.99994	0.99962	0.99938
0.3	0.98893	0.98384	0.98354	0.98330
0.5	0.92709	0.92137	0.92111	0.92089
0.7	0.77200	0.76323	0.76316	0.76297
0.9	0.43395	0.38967	0.38535	0.38584

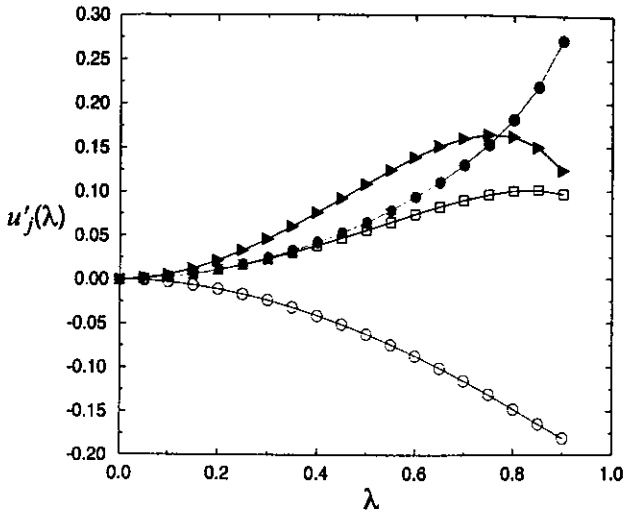

Fig. 2. Nonzero normalized velocity $u_j'(\lambda)$ versus the separation parameter $\lambda = a/h$. If $\zeta' = \zeta_1'$, then $j=3$ for Case 1 (□) and $j=1$ (○) for Case 2. If $\zeta' = \zeta_3'$, then $j=1$ (●) for Case 1 and $j=3$ (►) for Case 2.

dramatically affect the zero translation solution obtained for the single particle. As illustrated in Fig. 3, similar trends also hold for the nonzero-normalized velocity Ω_2': near the plane boundary Σ, the rotation of the sphere differs from the quantity $\Omega_2'(0)$. In addition, the difference $\Omega_2'(\lambda) - \Omega_2'(0)$ vanishes for only one specific value λ_0 in [0, 0.9] and is positive in one of the subdomains $[0, \lambda_0]$ or $[\lambda_0, 0.9]$ and negative in the other one.

In summary, Figs. 2 and 3 reveal that at least for the prescribed zeta potential functions ζ_1' and ζ_3', our wall effects are weak enough to be neglected as soon as the distance h roughly exceeds 10 times the radius a of the spherical particle. In case of a proximal boundary, wall–particle

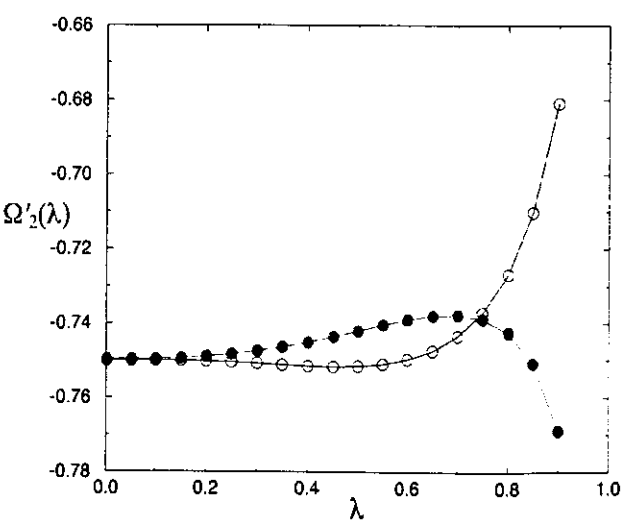

Fig. 3. Nonzero normalized velocity $\Omega_2'(\lambda)$ versus the separation parameter $\lambda = a/h$. For $\zeta' = \zeta_1'$ and for Case 2 (○). For $\zeta' = \zeta_3'$ and for Case 1 (●).

interactions may dramatically affect the solution that prevails for a single particle far from the boundary.

5. Conclusions

As clearly highlighted by the enclosed numerical results, wall effects on the electrophoretic motion of a nonuniformly charged sphere deeply depend upon both its zeta potential ζ (and the wall uniform zeta potential ζ_w for Case 1) and the applied electric field $\mathbf{E}_\infty$. Contrary to previous works in the field, the present approach not only circumvents the evaluation of the electrostatic potential and the electrolyte flow in the fluid domain but also makes it possible to cope with the general case of a nonspherical particle of the not necessarily uniform zeta potential distribution ζ. Future work will thereafter permit us to quantify nonsphericity and orientation effects in electrophoresis in proximity of a plane boundary. The case of the ellipsoidal particle is under current investigation and expected to bring some light on these basic issues. Finally, it is also worth noting that our boundary integral formulation is also likely to apply to challenging case of several particles.

References

[1] J.L. Anderson, Colloid transport by interfacial forces, Annu. Rev. Fluid Mech. 21 (1989) 61–99.
[2] M.V. Smoluchowski, in: L. Graetz (Ed.), Handbuch der Elektrizität und des Magnetismus, J.A. Barth, Leipzig, 1921, pp. 366–428.
[3] F.A. Morrison, Electrophoresis of a particle of arbitrary shape, J. Colloid Interface Sci. 34 (1970) 210–214.
[4] M. Teubner, The motion of charged colloidal particles in electric fields, J. Chem. Phys. 76 (11) (1982) 5564–5573.
[5] F.A. Morrison, J.J. Stuckel, Electrophoresis of an insulating sphere normal to a conducting plane, J. Colloid Interface Sci. 33 (1970) 88–103.
[6] H.J. Keh, J.L. Anderson, Boundary effects on electrophoretic motion of colloidal spheres, J. Fluid Mech. 153 (1985) 417–439.
[7] H.J. Keh, S.B. Chen, Electrophoresis of a colloidal sphere parallel to a dielectric plane, J. Fluid Mech. 194 (1988) 377–390.
[8] H.J. Keh, L.C. Lien, Electrophoresis of a colloidal sphere along the axis of a circular orifice or a circular disk, J. Fluid Mech. 224 (1991) 305–333.
[9] J.L. Anderson, Effect of nonuniform zeta potential on particle movements in electric fields, J. Colloid Interface Sci. 105 (1985) 45–54.
[10] M.C. Fair, J.L. Anderson, Electrophoresis of nonuniformly charged ellipsoidal particles, J. Colloid Interface Sci. 127 (1989) 388–400.
[11] J. Happel, H. Brenner, Low Reynolds Number Hydrodynamics, Martinus Nijhoff, Leyden, 1973.
[12] J.R. Blake, A note on the image system for a Stokeslet in a no-slip boundary, Proc. Cambridge Philos. Soc. 70 (1971) 303–310.